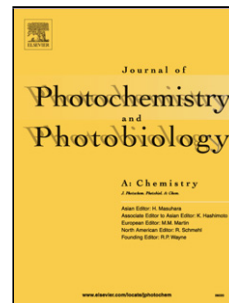


## Accepted Manuscript

Title: Benzimidazole and benzothiazole conjugated Schiff base as fluorescent sensors for Al<sup>3+</sup> and Zn<sup>2+</sup>

Authors: G.R. Suman, S.G. Bubbly, S.B. Gudennavar, V. Gayathri



PII: S1010-6030(19)30790-7  
DOI: <https://doi.org/10.1016/j.jphotochem.2019.111947>  
Article Number: 111947

Reference: JPC 111947

To appear in: *Journal of Photochemistry and Photobiology A: Chemistry*

Received date: 11 May 2019  
Revised date: 17 June 2019  
Accepted date: 19 June 2019

Please cite this article as: Suman GR, Bubbly SG, Gudennavar SB, Gayathri V, Benzimidazole and benzothiazole conjugated Schiff base as fluorescent sensors for Al<sup>3+</sup> and Zn<sup>2+</sup>, *Journal of Photochemistry and Photobiology, A: Chemistry* (2019), <https://doi.org/10.1016/j.jphotochem.2019.111947>

This is a PDF file of an unedited manuscript that has been accepted for publication. As a service to our customers we are providing this early version of the manuscript. The manuscript will undergo copyediting, typesetting, and review of the resulting proof before it is published in its final form. Please note that during the production process errors may be discovered which could affect the content, and all legal disclaimers that apply to the journal pertain.

# Benzimidazole and benzothiazole conjugated Schiff base as fluorescent sensors for $\text{Al}^{3+}$ and $\text{Zn}^{2+}$

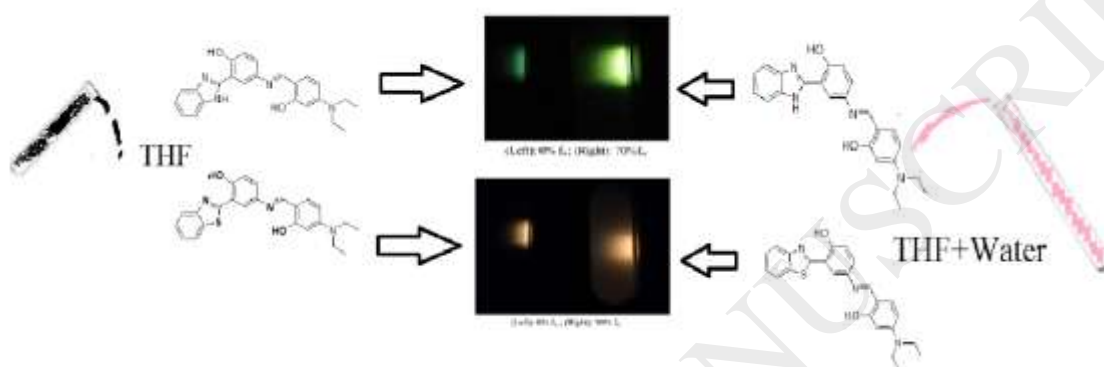
G. R. Suman<sup>a</sup>, S. G. Bubbly<sup>a\*</sup>, S. B. Gudennavar<sup>a</sup> and V. Gayathri<sup>b</sup>

<sup>a</sup> Department of Physics and Electronics, CHRIST (Deemed to be University), Bengaluru-560 029, Karnataka, India.

<sup>b</sup> Department of Chemistry, Bangalore University, Central College Campus, Bengaluru-560 001, Karnataka, India.

\*Correspondence to: S. G. Bubbly (e-mail: bubbly.sg@christuniversity.in)

## Graphical abstract



## Highlights

- Synthesis and photophysical behaviour of benzimidazoles /benzothiazoles.
- These fluorophores exhibit both ESIPT and AIE behaviour.
- Found to be sensitive and selective to  $\text{Al}^{3+}$  and  $\text{Zn}^{2+}$  metal ions.
- Large Stokes shift and high sensitivity makes them potential candidates for the detection of  $\text{Al}^{3+}$  and  $\text{Zn}^{2+}$ .

## Abstract

Two benzimidazole/benzothiazole based azomethines, (E)-2-(1H-benzo[d]imidazol-2-yl)-4-(4-(diethylamino)-2-hydroxybenzylideneamino)phenol (**HBZA**) and (E)-2-(benzo[d]thiazol-2-yl)-4-(4-(diethylamino)-2-hydroxybenzylideneamino)phenol (**HBTA**) were designed and synthesised. Investigations of solvatochromic behaviour of these fluorophores in solvents of varying polarities showed large Stokes shift of 134 - 210 nm. Time resolved Laser induced fluorescence measurements revealed the excited state dynamics of the fluorophores. Molecules were also found to be emissive in aggregated state as seen from the aggregation induced emission studies. Appreciable absorption and emission spectral changes upon co-ordination of **HBZA** with  $\text{Al}^{3+}/\text{Zn}^{2+}$  and **HBTA** with  $\text{Al}^{3+}$ , as well as good sensitivity and selectivity,

indicated their capability of detecting the two analytes. The binding stoichiometry was determined using electrospray ionization mass spectrometry (ESI-MS) and the binding mechanism was studied using density functional theory.

**Key words:** ESIPT, Schiff, Benzimidazole, AIE

## 1. Introduction

Fluorescent organic molecules having the characteristic properties of large Stokes shift, quick photo-response and appreciable photostability are ideal candidates for the fabrication of OLEDs, probes for recognition of chemical species, drug delivery applications etc. [1-5]. Understanding the photophysical and photochemical behaviour of such systems can help gain insight into their potential technological capabilities. The family of 2-(2'-hydroxyphenyl) benzimidazole, benzoxazole, benzothiazole and benzotriazole are known for their excited state intramolecular proton transfer (ESIPT) photo-tautomers with large Stokes shift [6-9]. Heterocyclic benzimidazole and benzothiazole derivatives have proved to be very good acceptors in D- $\pi$ -A structures due to their electron withdrawing nature [10, 11]. Their molecular structures can be tailored through conjugation with proton donating moieties for larger Stokes shift as well as high quantum yield [12, 13]. Fluorescence and self-assembling properties of benzimidazole/benzothiazole derivatives have been exploited for their pronounced fluorescence through aggregation induced emission (AIE), a phenomenon having applications in bioimaging, optoelectronics and chemosensors [14, 15]. Moreover, organic fluorescent molecules featuring large Stokes shift, quantum yield and binding multiple analytes with effective sensitivity and selectivity are explored as chemosensors for metal ion sensing [16-20].

In recent years, chemosensors for biologically and environmentally important species have gained much attention. Among the various metal ions, aluminium ( $\text{Al}^{3+}$ ) is the third most abundant element in the earth's crust and because of its diverse applications in our everyday life, there are myriad ways in which humans are exposed to aluminium. Accumulation of Al in the body can cause anaemia, neural and Alzheimer's disease [21, 22]. However, zinc ( $\text{Zn}^{2+}$ ) is a biologically indispensable trace element playing significant structural, catalytic and regulatory roles in physiological processes [23-25]. Any imbalance in  $\text{Zn}^{2+}$  causes various health issues as the deficiency or excess of it would lead to undergrowth, diarrhoea, Parkinson's disease and other neurological disorders like Alzheimer's, amyotrophic lateral sclerosis and epilepsy [26, 27]. Hence monitoring  $\text{Al}^{3+}$  and  $\text{Zn}^{2+}$  is of great concern. A combination of two or more emission phenomena such as intramolecular charge transfer (ICT) - photoinduced electron transfer (PET), ICT-ESIPT, ESIPT-AIE can be used to obtain multiple signals to sense various analytes simultaneously [28]. In the present work, we have investigated the fluorescence behaviour of two systems with dual ESIPT sites and diethyl amine moiety which can act as charge transferring unit. We have synthesized (E)-2-(1H-benzo[d]imidazol-2-yl)-4-(4-(diethylamino)-2-hydroxybenzylideneamino)phenol (**HBZA**) and (E)-2-(benzo[d]thiazol-2-yl)-4-(4-(diethylamino)-2-hydroxybenzylideneamino)phenol (**HBTA**) and studied their

ESIPT-AIE properties. Furthermore, **HBZA** was capable of detecting  $\text{Al}^{3+}$  and  $\text{Zn}^{2+}$  with micromolar sensitivity at two different wavelengths and **HBTA** could sense  $\text{Al}^{3+}$ , over other metal ions. Computational analysis was carried out using Gaussian 09 software to understand the sensing mechanism [29].

## 2. Experimental

### 2.1 Materials and methods

All solvents (HPLC grade) were used as procured from Alfa Aesar. Chemicals were purchased from Sigma Aldrich. UV-Visible absorption and fluorescence emission spectra were recorded using Shimadzu UV-1800 and Shimadzu RF-5301 PC spectrometers respectively. Fluorescence emission was recorded at the excitation and emission slit widths of 3 nm. Absolute quantum yields were measured using calibrated integrating sphere incorporated in Horiba Jobin Yvon Fluoromax-4 spectrofluorimeter. Time resolved fluorescence decay measurements were carried out using Horiba Jobin Yvon Fluorocube -01-NL Fluorescence Life time System. Photons with 10 MHz repetition rate were generated using LASER (D-405L for **HBZA**) and LED (DD-340) excitation sources and DAS6 software was used to analyse the data. Dynamic light scattering measurements for particle size determination were performed on Brookhaven ZetaPALS potential analyser.  $^1\text{H}$  NMR spectra were recorded on Bruker AC400 spectrometer in  $\text{DMSO-d}_6$ . LC-MS data were obtained using Shimadzu spectrometer equipped with Ascentis Express C18 ( $50\text{ mm} \times 2.1\text{ mm} \times 2.7\text{ }\mu\text{m}$ ) column with mobile phase A: 0.1% formic acid in water and mobile phase B: ACN. ESI-MS data for understanding binding stoichiometry was recorded on Agilent technologies LC-1200 series and MS-6130 Quadrapole with C18 ( $4.6\text{ mm} \times 0.75\text{ mm}$ ) column using mobile phase A: 0.1% formic acid in water and mobile phase B: ACN. Theoretical calculations using density functional theory (DFT) were carried out at B3LYP/6-31G(d,p) levels for C, H, N, O and S atoms and LanL2dz for metal ions using Gaussian 09 software.

### 2.2 Synthesis of 4-amino-2-(1H-benzimidazol-2-yl)phenol (**HBZ**) and 4-amino-2-(benzothiazol-2-yl)phenol (**HBT**)

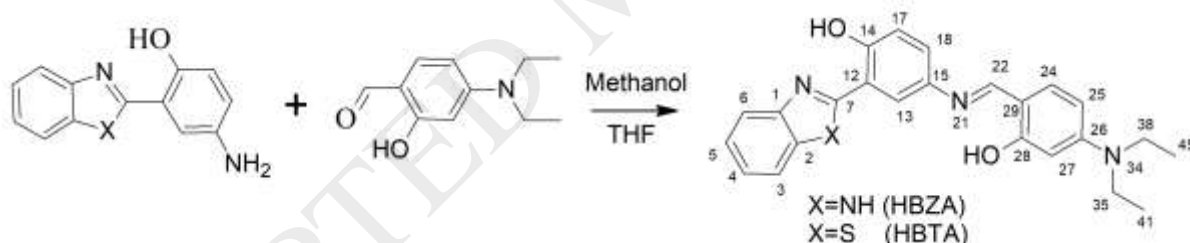
**HBZ** and **HBT** were synthesized according to the procedure reported by Hein et al. [30]. **HBZ** was prepared by heating equimolar ratio of 1,2-phenylenediamine (1.08 g, 0.01 mol) and 5-amino-2-hydroxybenzoic acid (1.37 g, 0.01 mol) at  $160\text{ }^\circ\text{C}$  for 8 hours in 3.5 mL polyphosphoric acid. After the completion of the reaction (as indicated by the TLC analysis of small aliquot) the reaction mixture was quenched in ice and neutralized using 10%  $\text{Na}_2\text{CO}_3$  solution. Excess base was removed by washing with ice-cold water. The precipitate was dried overnight and recrystallized in methanol to obtain 4-amino-2-(1H-benzimidazol-2-yl)phenol (**HBZ**). Similarly, 4-amino-2-(benzothiazol-2-yl)phenol (**HBT**) was synthesized by using 2-aminothiophenol.

### 2.3 Synthesis of (E)-2-(1H-benzo[d]imidazol-2-yl)-4-(4-(diethylamino)-2-hydroxybenzylideneamino) phenol (HBZA) and (E)-2-(benzo[d]thiazol-2-yl)-4-(4-(diethylamino)-2-hydroxybenzylideneamino)phenol (HBTA)

**HBZA** and **HBTA** were obtained from **HBZ** and **HBT** respectively, by adopting the following synthesis procedure. Progress of reactions were monitored by TLC analysis of reaction mixtures at regular intervals.

**HBZ** (100 mg, 0.44 mmol) was refluxed with 4-(diethylamino)-2-hydroxybenzaldehyde (85 mg, 0.44 mmol) in 10 mL methanol for 8 hours. Yellow solid obtained was purified by column chromatography to yield (E)-2-(1H-benzo[d]imidazol-2-yl)-4-(4-(diethylamino)-2-hydroxybenzylideneamino) phenol (**HBZA**) (Scheme 1; X=NH). Yield: 150 mg, 81%. <sup>1</sup>H NMR (SFig. 1a)  $\delta$  in ppm: 13.21 (s, 1H), 8.75 (s, 1H), 8.10 (d, 2H), 7.69 (s, 1H), 7.48-7.30 (m, 3H), 7.10 (d, 8.8 Hz, 1H), 6.35 (d, 8.8 Hz, 1H), 6.08 (dd, 2.4 Hz, 1H), 3.41 (dd, 7.2 Hz, 4H), 1.359 (s, 1H), 1.17 (t, 6H). LC-MS (SFig. 2a): Calc. for C<sub>20</sub>H<sub>15</sub>N<sub>3</sub>O<sub>2</sub>:400.2; found: 400.0.

**HBT** (100 mg, 0.41 mmol) was refluxed with 4-(diethylamino)-2-hydroxybenzaldehyde (79 mg, 0.41 mmol) in 10 mL Tetrahydrofuran (THF) for 8 hours. Reaction mixture was concentrated on water bath and the product obtained was purified by column chromatography which yielded green solid of (E)-2-(benzo[d]thiazol-2-yl)-4-(4-(diethylamino)-2-hydroxybenzylideneamino)phenol (**HBTA**) (Scheme 1; X=S). Yield: 155 mg, 87%. <sup>1</sup>H NMR (SFig. 1b)  $\delta$  in ppm: 13.79 (s, 1H), 13.38 (s, 1H), 9.85 (1s, 1H), 8.20 (d, 2H), 7.52-7.30 (m, 4H), 6.88 (d, 8.4 Hz, 1H), 6.01 (dd, 0.8 Hz, 2H), 3.559 (dd, H) LC-MS (SFig. 2b): Calc. for C<sub>20</sub>H<sub>15</sub>N<sub>3</sub>O<sub>2</sub> [M+H<sup>+</sup>]: 420.2 Found: 420.2.



**Scheme 1.** Synthesis of **HBZA** and **HBTA**

### 2.4 UV-Vis absorption and fluorescence studies

Absorption and emission spectra were recorded in solvents ( $10^{-5}$  M) of varying polarities for **HBZA** and **HBTA**. Fluorescence sensing measurements were performed by dissolving **HBZA** and **HBTA** in DMF/water ( $10^{-4}$  M in 9:1 v/v) and THF/water ( $10^{-4}$  M in 9:1 v/v) mixed solvents respectively.  $10^{-3}$  M aqueous metal ion solutions were prepared using nitrate salts of K, Zn, Sr, Ni, Ba, Al, Pb, and chloride salts of Mn, Mg, Hg, Cu and Cd. pH adjustments for ion sensing were carried out using buffer solutions of Na<sub>2</sub>CO<sub>3</sub> and H<sub>3</sub>PO<sub>4</sub>. Effect of competitive ions on absorption and emission spectra were recorded using  $10^{-4}$  M solutions of fluorophores and  $10^{-3}$  M solutions of interfering ions. Analyte solutions ( $10^{-4}$  M) were prepared at 7.2 pH in water. Detection limit and binding constants were obtained from

fluorescence spectral measurements of  $10^{-4}$  M **HBZA** and **HBTA** in presence of varying concentrations,  $(0 - 30) \times 10^{-5}$  M, of analytes. Limit of detection was calculated according to  $(3\sigma/s)$ , where  $\sigma$  the standard deviation of blank sample and  $s$  is slope of the fluorescence emission intensity versus metal ion concentration. Binding constants were determined according to modified Benesi-Hildebrand equation (Supplementary information) according to the reported procedure [22, 31, 32]. Aggregation induced emission studies were carried out for **HBZA** in DMF/water and **HBTA** in THF/water. Stock solutions of **HBZA** and **HBTA** were prepared at  $10^{-3}$  M concentration in 5 mL DMF and THF respectively and further diluted by adding varying water fractions ( $f_w = 0$  to 90%) to get  $10^{-4}$  M solutions. Aggregation was confirmed by dynamic light scattering (DLS) method and average diameter of the particles was determined using Brookhaven ZetaPALS potential analyser.

### 3. Results and discussion

#### 3.1 UV-visible absorption and fluorescence spectroscopic studies

Absorption spectra of **HBZA** (Fig. 1a) showed variation in absorption wavelength depending on the hydrogen bonding ability of the solvent. However, there was not much variation observed for **HBTA**, except in THF and dichloromethane (DCM), where the absorption wavelengths showed a red shift of 31 and 32 nm respectively with respect to methanol (Fig. 2a). This indicates that **HBZA** is more sensitive to solvent environment than **HBTA**, in ground state. Interestingly fluorescence emission in **HBZA** (Fig. 1b) has only single peak in all the solvents. This was also supported by excited state life time measurement in

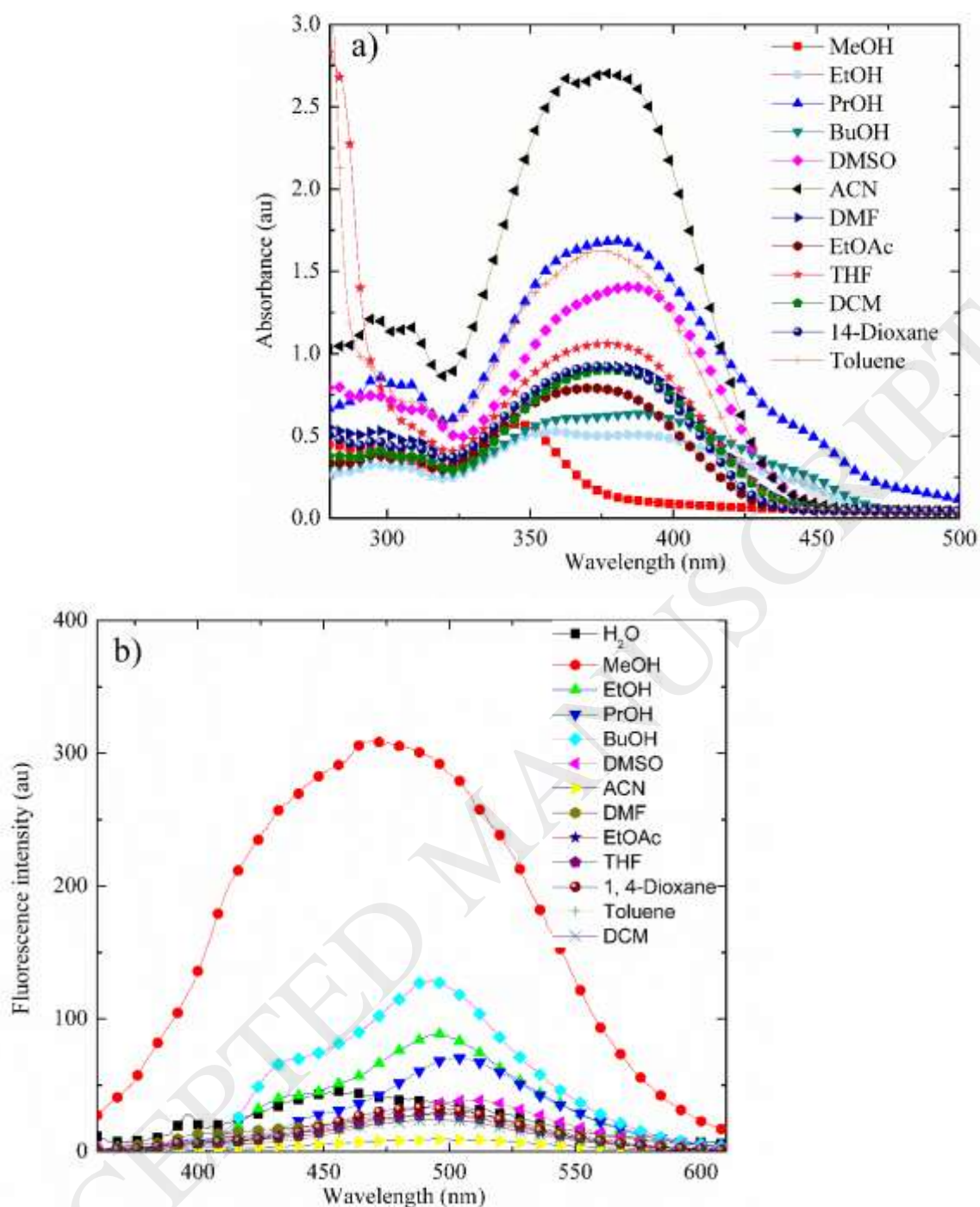


**Fig. 1.** a) Absorption and b) fluorescence emission spectra of **HBZA** in various solvents

methanol. Time resolved fluorescence decay measurement of **HBZA** excited at 405 nm and monitored at 500 nm showed a single species with life time of  $3.47 \times 10^{-11}$  s (77%) (SFig. 3). **HBZA** and **HBTA** in water have also showed similar variations in Stokes shift as exhibited in polar solvents. Steady state fluorescence spectra in case of **HBTA** exhibited dual emissions (Fig. 2b) along with a large Stokes shift of 210 nm in THF (STable 1). Another interesting feature of **HBTA** is that its emission spectra at 586 nm in THF and DCM have shown yellowish-orange, faint and bright emissions respectively, suggesting colour tunability of

**HBTA.** Intense emission with large Stokes shift in non-polar solvent like DCM and the large Stokes shift even in hydrogen bonding solvent like water suggests the ICT- coupled ESIPT emission characteristics of HBTA. The life time measurements with excitation wavelength of 345 nm also showed dual exponential decay with life time of  $1.28 \times 10^{-11}$  s (75%) for the peak at 436 nm (SFig. 4a) and 5.99 ns (36%) and 0.11 ns (37%) when monitored at 506 nm (SFig. 4b). HBZA showed more quantum yield of 0.4 compared to that of HBTA (0.09). This was also supported by large non- radiative constant value of HBTA compared to HBZA (STable 2). Charge distribution on frontier molecular orbitals (FMOs) calculated using DFT can be used to understand the nature of transition from ground to excited state. FMOs such as LUMO and LUMO+1 level in case of **HBZA** were formed mainly due to the delocalized charges, however for **HBTA** charges are localized on benzothiazole in LUMO and on diethylamino salicylidene unit in LUMO+1 level. HOMO levels in both **HBZA** and **HBTA** were contributed by phenyl-diamino salicylidene (Figs. 3 and 4). These studies indicate that charge transfer characteristics are more dominant in **HBZA**.

### 3.2 Aggregation induced emission studies

**HBZA** showed decrease in absorbance (SFig. 5a) and increase in intensity of emission (Fig. 5a) with successive addition of water to THF. The emission intensity at 506 nm reached a maximum (104-fold enhancement) at 70%  $f_w$ , with a blue shift of 23 nm with respect to THF. **HBTA** also showed similar variation in absorption (SFig. 5b). The fluorescence intensity at 587 nm showed 8-fold enhancement for 90%  $f_w$  compared to 0%  $f_w$  (Fig. 5b) with negligible red shift (3 nm). Average particle diameter was determined using ZetaPals analyser for 60 - 80%  $f_w$  solutions of **HBZA** and 70 - 90%  $f_w$  solutions of **HBTA** (STable 3). Enhancement in emission in the aggregated state may be attributed to restriction of  $\pi$ - $\pi$  stacking due to the twisted structure of **HBZA** and **HBTA** observed from DFT optimization (SFig. 6).

### 3.3 Absorption and fluorescence sensing of HBZA and HBTA in different metal ions

Optical response of **HBZA** towards various metal ions showed notable changes in absorption wavelength for  $Zn^{2+}$  and  $Al^{3+}$  compared to other ions (Fig. 6a). Binding of analyte with **HBZA** was evident from the 10 nm red shift for  $Zn^{2+}$  (Fig. 6a) and 25 nm blue shift for  $Al^{3+}$  (Fig. 6a) complexes. In case of fluorescence emission, a blue shift of 46 nm with 19-fold enhancement in intensity at 495 nm was observed for **HBZA**-  $Zn^{2+}$  complex (Fig. 6b). Interaction of  $Al^{3+}$  with **HBZA** resulted in a 62 nm blue shift in emission with a 7-fold increase in intensity at 479 nm (Fig. 6b). Binding stoichiometry was obtained based on Job's plot analysis by using fluorescence emission spectra. Individual addition of different mole fractions (0 - 9) of  $Zn^{2+}$  and  $Al^{3+}$  to **HBZA** showed a binding ratio of 0.5:1 for  $Zn^{2+}$ : ligand (SFig. 7a) and 2:1 for  $Al^{3+}$ : ligand (SFig. 7b). Binding stoichiometry was also confirmed by ESI-MS spectral analysis. ESI-MS spectrum of  $Zn^{2+}$ :**HBZA** showed m/z at 526.7 due to  $[Zn + \mathbf{HBZA} + NO_3]^+$ , calculated: 526.1, suggesting 1:1 stoichiometry for  $Zn^{2+}$ -**HBZA** (SFig. 8a). For  $Al^{3+}$ -**HBZA**, ESI-MS exhibited m/z at 640.1 corresponding to the mass of  $[Al_2 + \mathbf{HBZA} + (NO_3)_2 + HCOOH + H_2O]^+$ , calculated: 640.13, suggesting 2:1 binding ratio for  $Al^{3+}$ -**HBZA** (SFig. 8b).

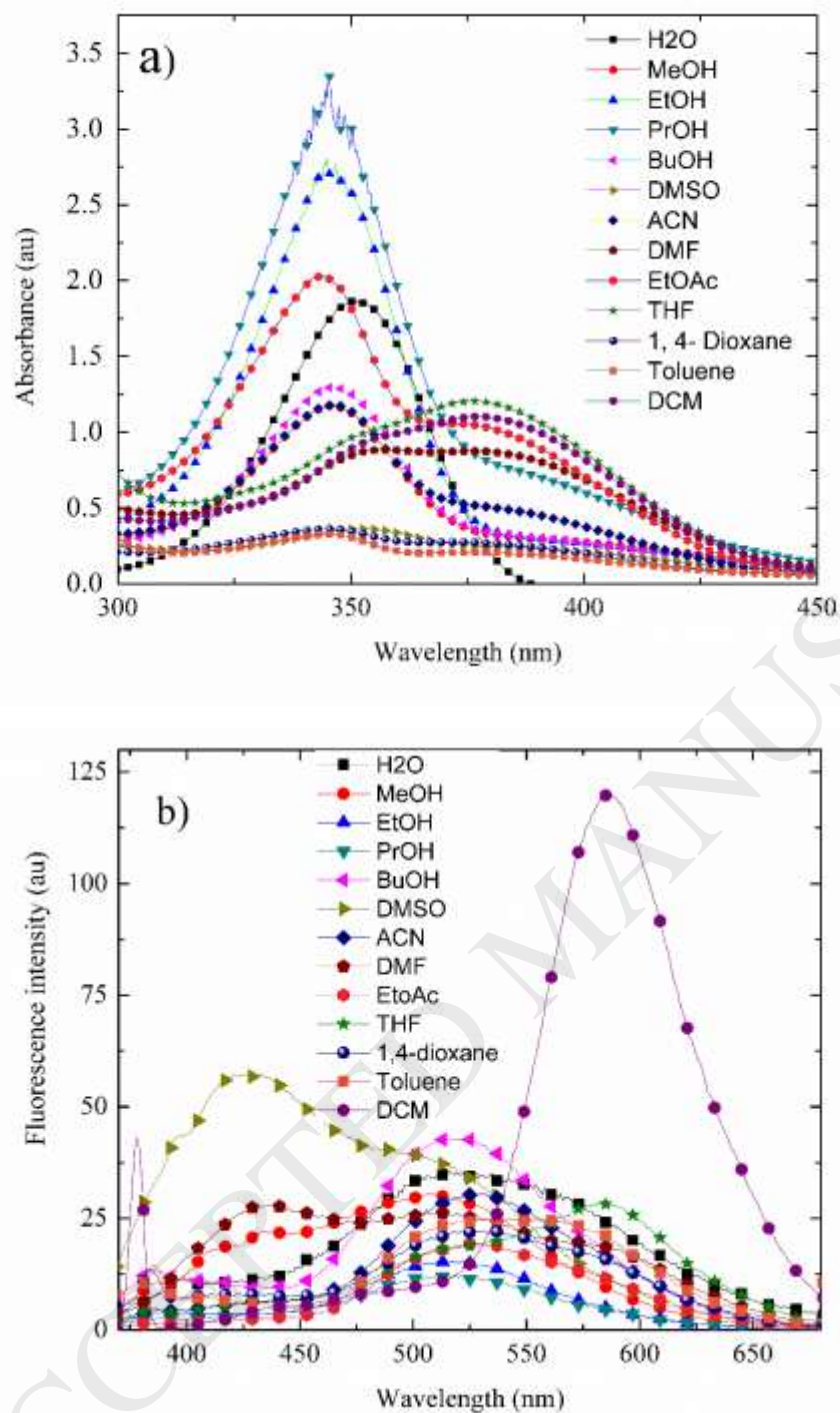


**Fig. 2.** a) Absorption and b) fluorescence emission spectra of **HBTA** in various solvents

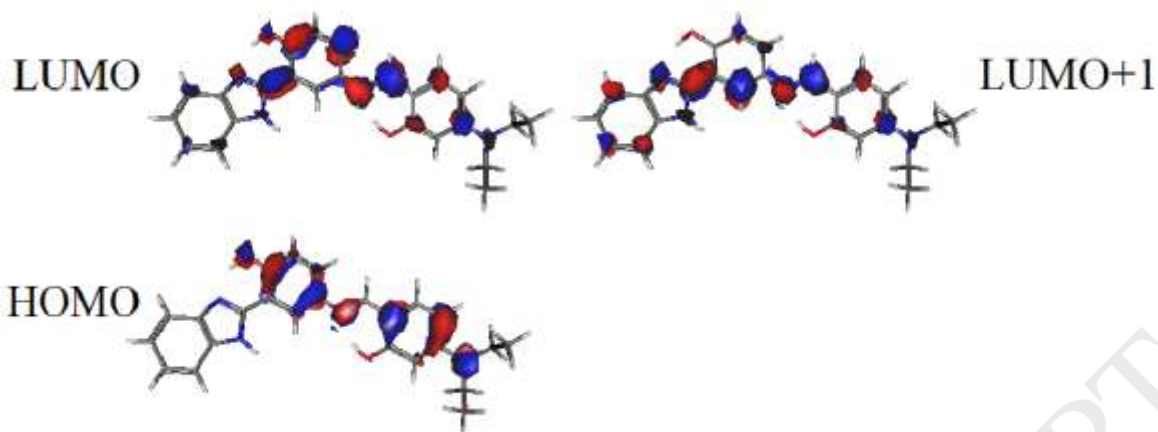


**Fig. 3.** Frontier molecular orbitals of **HBZA**

**HBTA** also exhibited absorption and emission spectral response for  $\text{Al}^{3+}$  different from all other ions. Complex formation resulted in 28 nm blue shift in absorbance (Fig. 7a) and a large hypsochromic shift of 82 nm in fluorescence emission with a 3-fold enhancement in emission intensity at 503 nm (Fig. 7b). Job's plot for **HBTA** showed a binding ratio of 1.5:1 for  $\text{Al}^{3+}$ : ligand (SFig. 7c). ESI-MS spectrum showed ion peak at 638.7 due to  $[\text{Al}_2 + \text{HBTA} + (\text{NO}_3)_2 + \text{HCOOH}]^+$ , calculated: 639.08, suggesting 2:1 binding stoichiometry for  $\text{Al}^{3+}$ :**HBTA** (SFig. 8c).

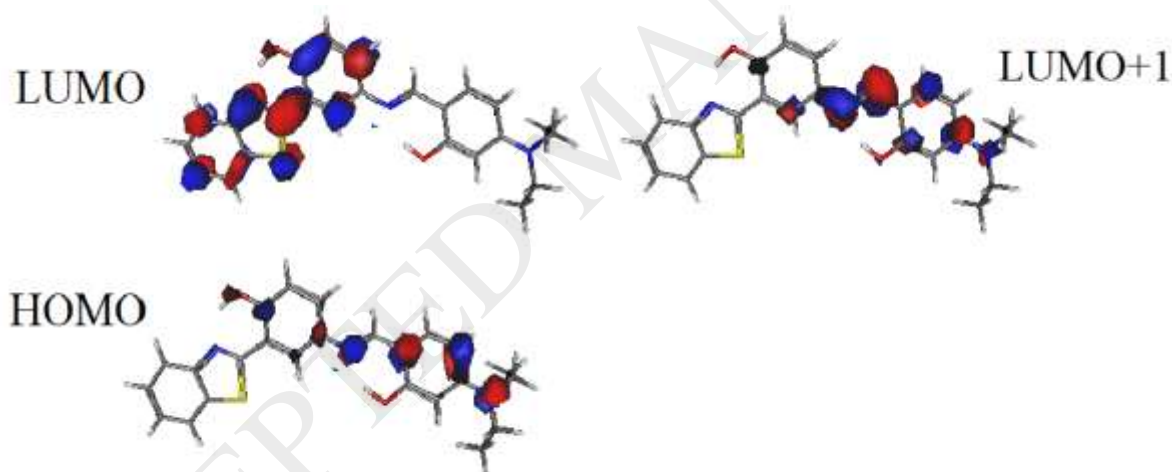


**Fig. 4.** Frontier molecular orbitals of **HBTA**

The sensing potential of **HBZA** was studied by titration of  $10^{-4}$  M receptor against varying concentrations of  $\text{Zn}^{2+}$  and  $\text{Al}^{3+}$  and the limits of detection (LOD) were found to be 0.21  $\mu\text{M}$  (Fig. 8a) and 0.11  $\mu\text{M}$  (Fig. 8b) respectively. Sensitivity studies on **HBTA** showed a detection limit of 0.87  $\mu\text{M}$  (Fig. 8c) for  $\text{Al}^{3+}$ . Metal ion sensing ability for both the fluorophores were very much below the permissible level of  $\text{Al}^{3+}$  and  $\text{Zn}^{2+}$  ions in drinking water as specified by WHO [22, 33, 34]. **HBZA** and **HBTA** provide better sensitivity for the respective metal ions when compared to the analogues of these fluorophores [35-37] suggesting the importance of **HBZA** and **HBTA** for sensing applications. Binding constants ( $K_a$ ) were found to be  $3.42 \times 10^2 \text{ M}^{-1}$  for  $\text{Zn}^{2+}$ -**HBZA** (Fig. 9a),  $2.25 \times 10^8 \text{ M}^{-2}$  for  $\text{Al}^{3+}$ -**HBZA** (Fig. 9b) and  $2.15 \times 10^8 \text{ M}^{-2}$  for  $\text{Al}^{3+}$ -**HBTA** (Fig. 9c).

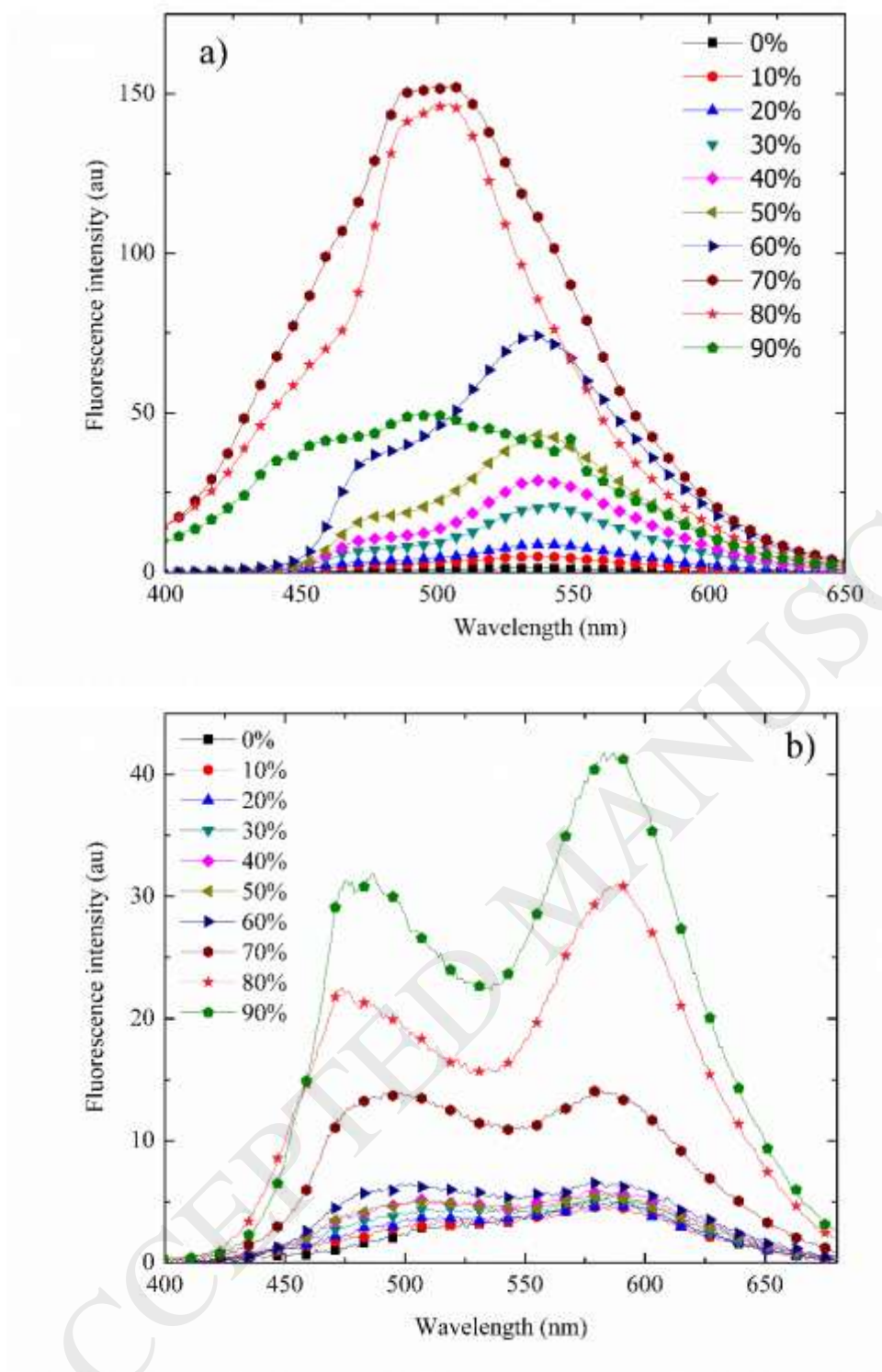


**Fig. 5.** Fluorescence emission of a) HBZA and b) HBTA in various water fractions (0 - 90%)

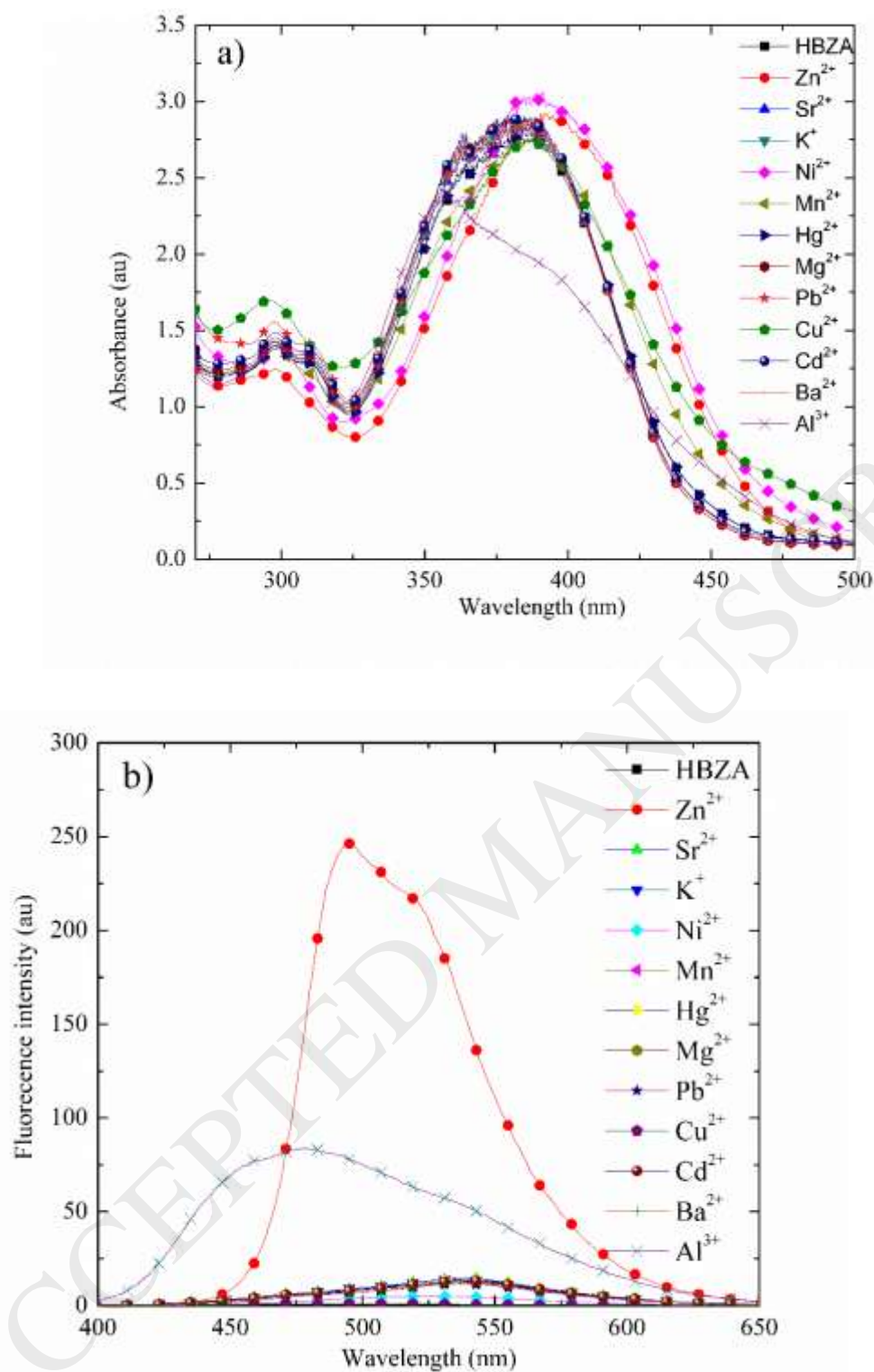
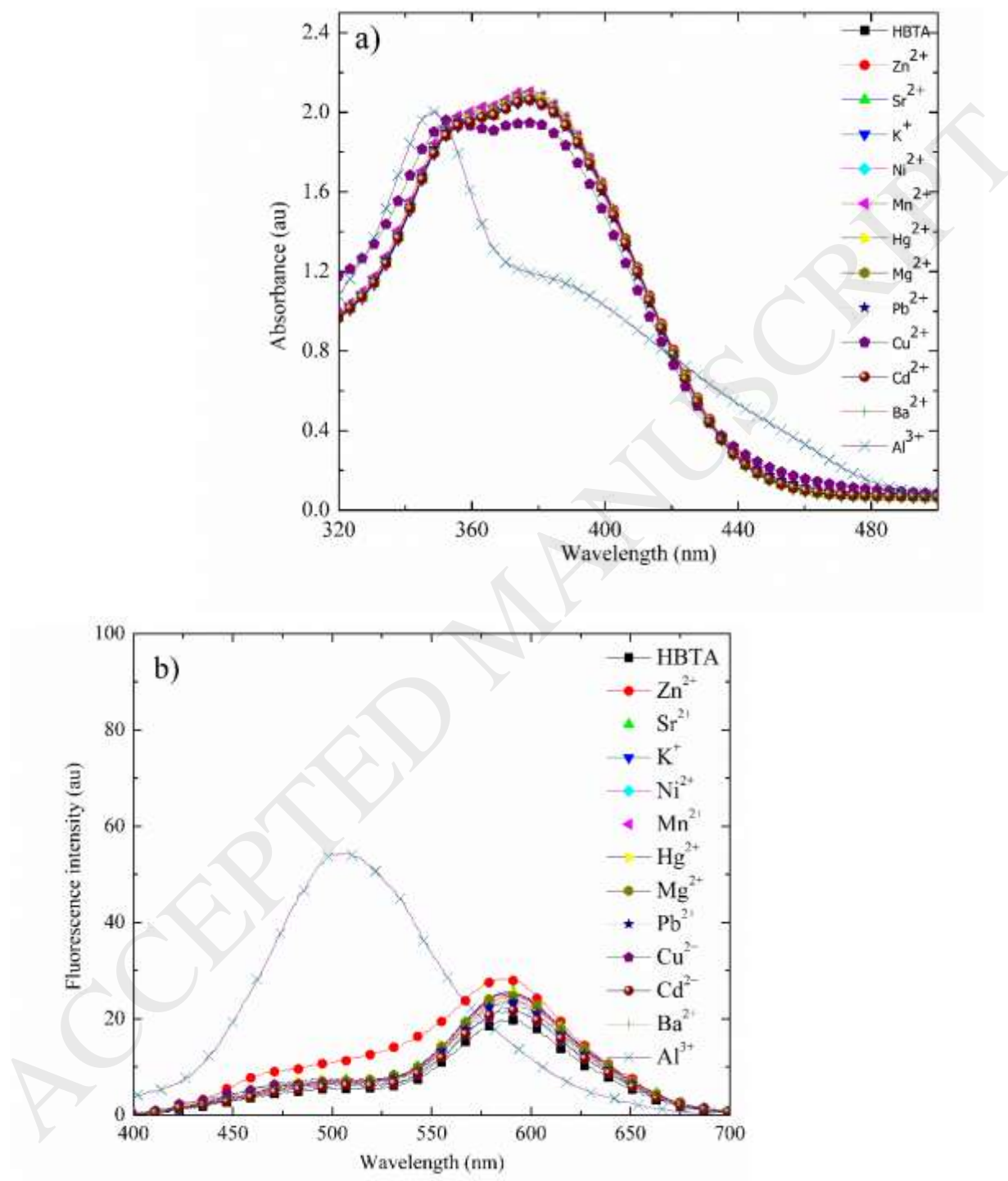


**Fig. 6.** a) Absorption and b) emission spectra of metal ions with **HBZA**

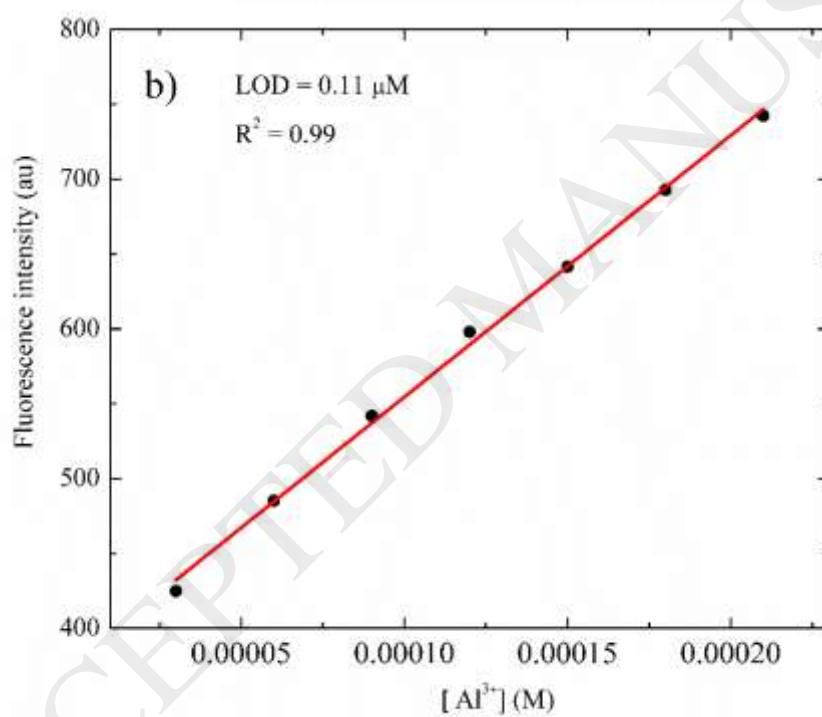
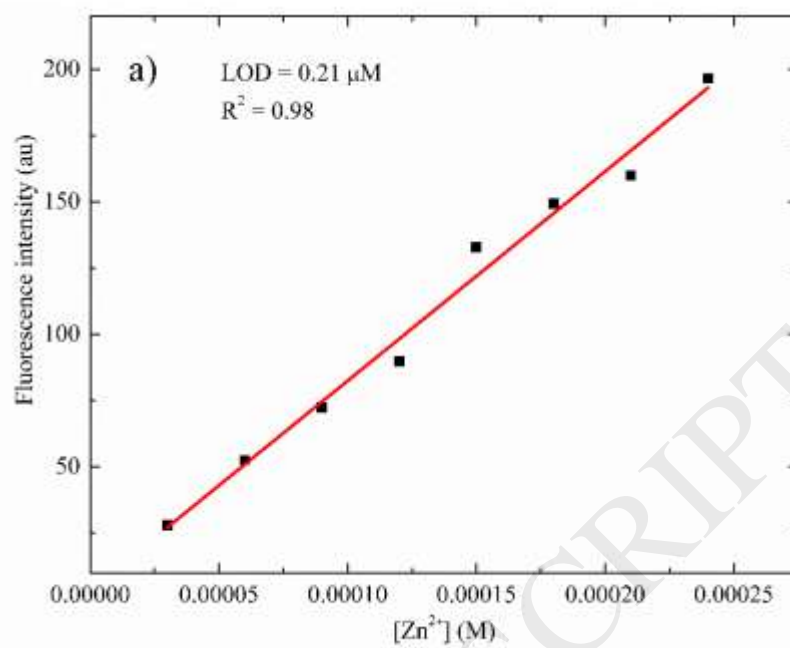
### 3.3.1 Interference effect of competitive metal ions

Effect of competitive ions on the emission from complexes was evaluated by recording emission spectra of 1 equivalent of Zn<sup>2+</sup> and Al<sup>3+</sup> in **HBZA** and adding a higher concentration (10 equivalents) of competitive ions. Turn on emissions of **HBZA-Zn<sup>2+</sup>** (Fig. 10) and Al<sup>3+</sup> complex (Fig. 11) being

unaltered in the presence of competitive ions (except for a moderate response from strong quencher  $\text{Cu}^{2+}$ ), indicated that **HBZA** can be utilized for sensing  $\text{Zn}^{2+}$  and  $\text{Al}^{3+}$ . In the case of **HBTA**- $\text{Al}^{3+}$ , none of the competitive ions hampered the emission, indicating **HBTA** to be highly selective towards  $\text{Al}^{3+}$  ions (Fig. 12).



**Fig. 7.** a) Absorption and b) emission spectra of **HBTA** in presence of various metal ions



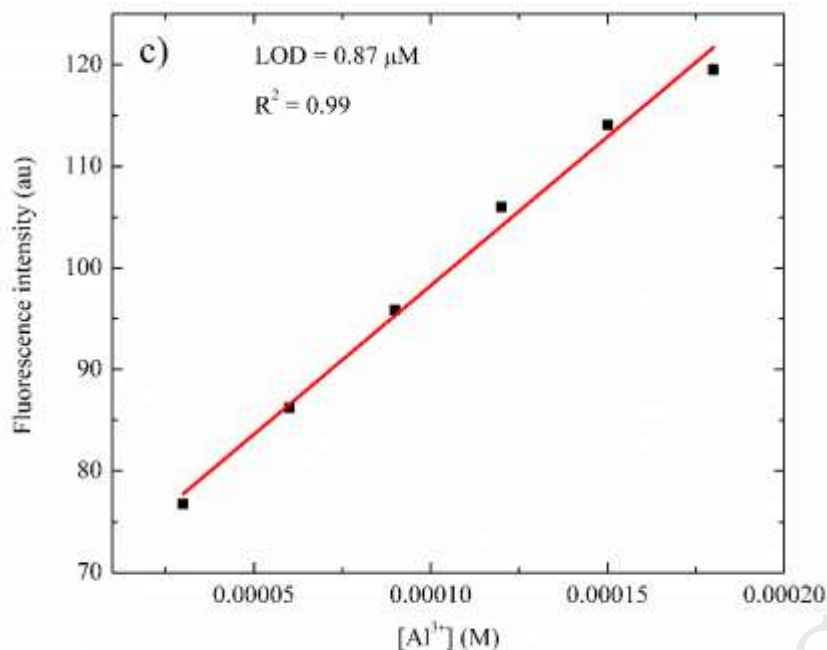
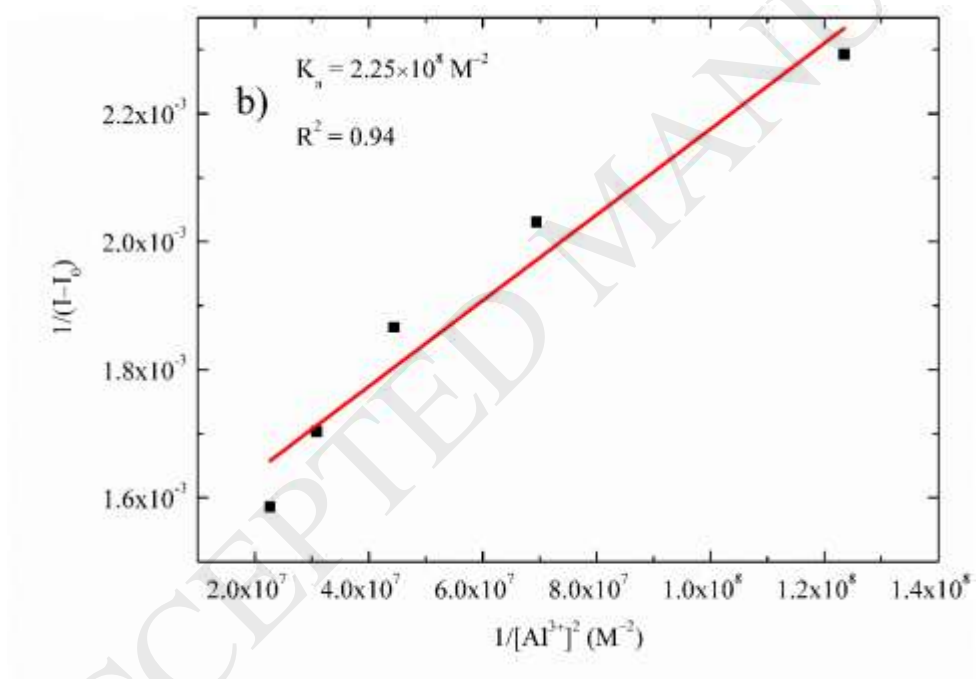
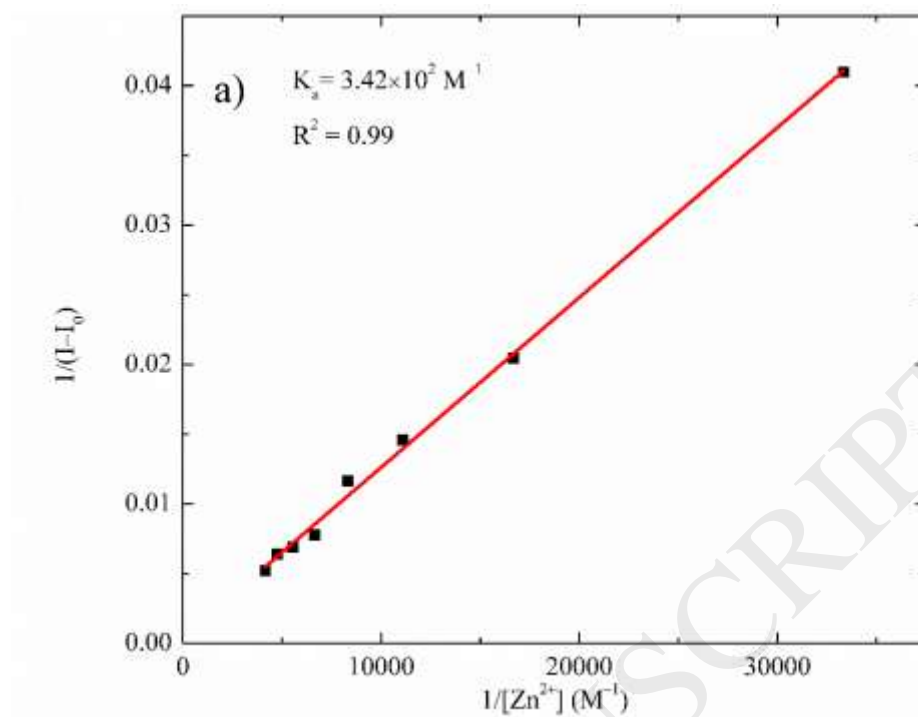


Fig. 8. Sensitivity of **HBZA** towards a)  $\text{Zn}^{2+}$  and b)  $\text{Al}^{3+}$  and c) **HBTA** towards  $\text{Al}^{3+}$

### 3.4 Computational studies using Gaussian 09

DFT calculations were carried out to study the sensing mechanism. Conjugation of **HBZA** and **HBTA** with  $\text{Al}^{3+}$  resulted in the reduction in HOMO and LUMO levels, whereas it was increased in case of  $\text{Zn}^{2+}$ -**HBZA** (Table 1). Complex formation was also evident from the reduced band gap of the complex compared to the ligands. Charge distribution pattern in the complex in HOMO and LUMO levels were obtained from frontier molecular orbitals analysis. In **HBZA**- $\text{Al}^{3+}$  complex, nitrogen on the Schiff base acts as the binding site resulting in the suppression of ESIPT. This was supported by the delocalized charge distribution observed in LUMO level (SFig. 9a). In case of **HBZA**- $\text{Zn}^{2+}$ , oxygen and nitrogen atoms on salicylidene ring have acted as platforms for chelation of  $\text{Zn}^{2+}$ . While the contribution for HOMO level was from the entire molecule, as observed from the delocalized charges, the LUMO level was due to charge transfer from the ligand to metal (LMCT) bound to salicylidene unit (SFig. 9b). In **HBTA**- $\text{Al}^{3+}$ , the charge transfer was observed from the salicylidene ring (HOMO) to the benzothiazole unit (LUMO) (SFig. 9c). Co-ordination of  $\text{Al}^{3+}$  with **HBZA** has manifested in a slightly twisted structure.  $\text{Zn}^{2+}$ -**HBZA** complex exhibited a more planar structure (which supports the red shift observed in absorption wavelength). **HBTA**- $\text{Al}^{3+}$  complex also exhibited a slightly twisted conformation compared to **HBTA** (Table 2).



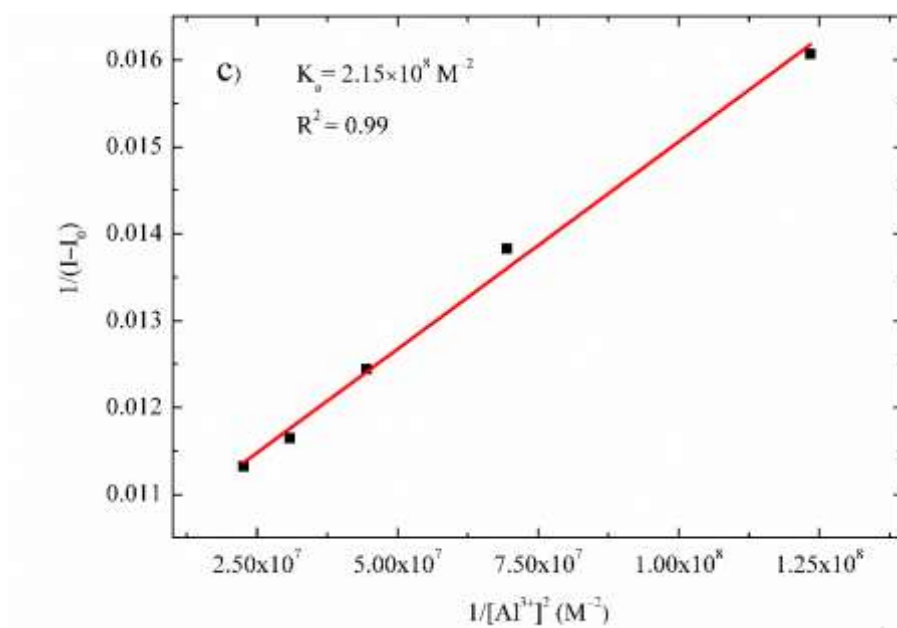


Fig. 9. Benesi-Hildebrand plot for a) **HBZA**-Zn<sup>2+</sup>, b) **HBZA**-Al<sup>3+</sup> and c) **HBTA**-Al<sup>3+</sup>

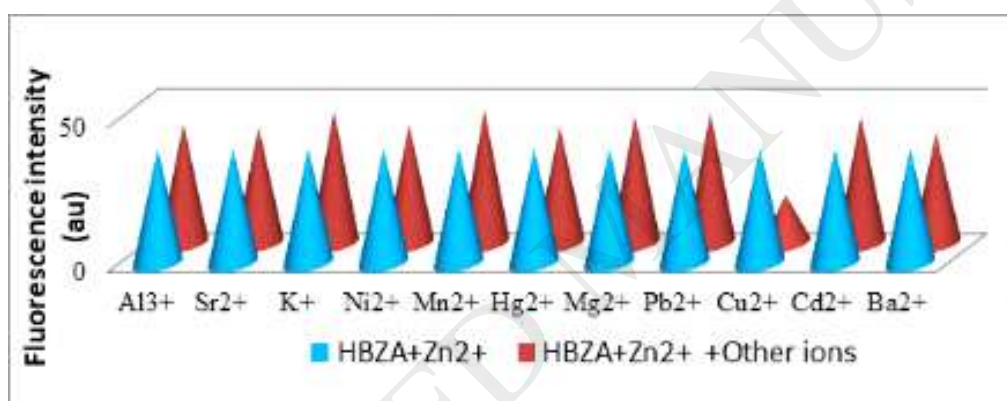


Fig. 10. Selectivity of **HBZA** for Zn<sup>2+</sup> in presence of competitive ions.

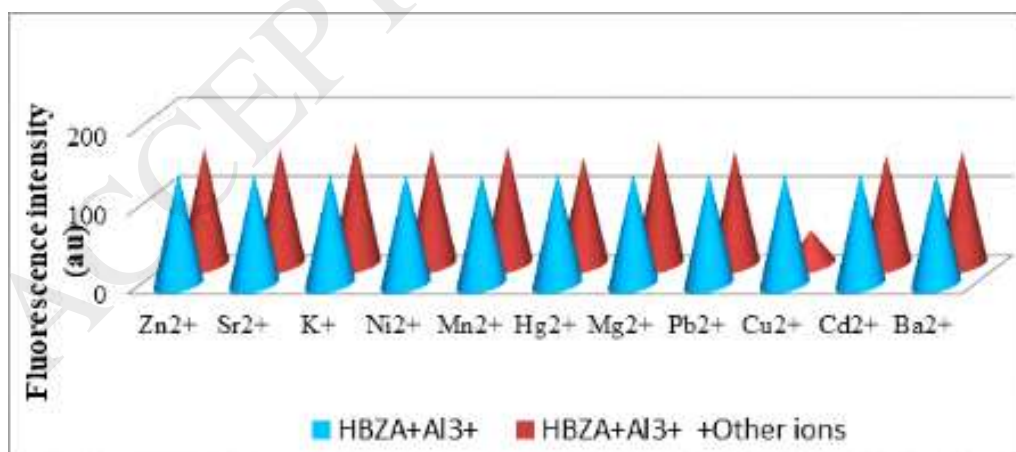
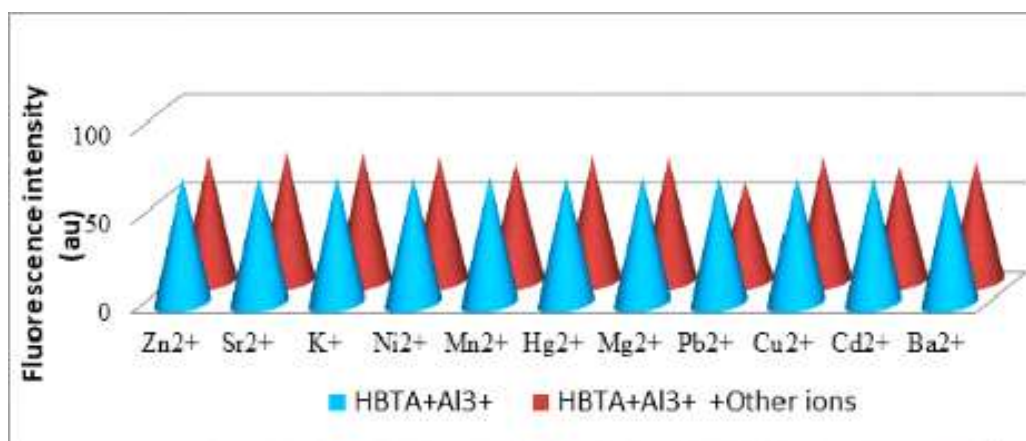


Fig. 11. Selectivity of **HBZA** for Al<sup>3+</sup> in presence of competitive ions.



**Fig. 12.** Selectivity of **HBTA** for  $\text{Al}^{3+}$  in presence of competitive ions.

**Table 1.** Energy level comparison obtained from DFT calculations

Molecule	HOMO (eV)	LUMO (eV)	Bandgap (eV)
HBZA	-5.55	-1.57	3.98
HBZA- $\text{Al}^{3+}$	-3.09	-1.27	1.82
HBZA- $\text{Zn}^{2+}$	-5.94	-2.96	2.98
HBTA	-4.97	-1.66	3.31
HBTA- $\text{Al}^{3+}$	-3.0	-1.65	1.35

**Table 2.** Dihedral angles ( $^\circ$ ) obtained using DFT

Compound	Ligand dihedral angle	Dihedral angle with $\text{Al}^{3+}$	Dihedral angle with $\text{Zn}^{2+}$
HBZA (C15-N21-C22-C29)*	177.322	173.187	179.530
HBTA (C15-N21-C22-C24)*	177.245	174.737	---

\* Refer scheme 1

## 4. Conclusions

Fluorophores, **HBZA** and **HBTA**, exhibiting large Stokes shift and aggregation induced emission behaviour were designed and synthesized by reflux reaction from **HBZ** and **HBT**. The solvatochromic interaction was studied to understand sensitivity of probes for various polarities of the solvents. DFT studies and solvatochromic studies showed that **HBZA** followed ICT characteristics whereas ESIPT was more probable in **HBTA**. The probes were found to exhibit aggregation induced emission. Metal ions sensing studies suggest that **HBZA** was able to detect  $\text{Al}^{3+}$  and  $\text{Zn}^{2+}$ . Spectral response of **HBTA** towards various ions showed turn on emission for  $\text{Al}^{3+}$  with no interaction with any other ion. Both the fluorophores were found to be very much sensitive towards the metal ions with sensitivity very much lower than that specified by WHO. The probes were also more selective towards the analytes in presence of competitive ions.

### Acknowledgements

The authors would like to thank the anonymous reviewers for their valued comments and suggestions, which greatly helped in improving the quality of the manuscript.

### References

- [1] H. Liu, X. Cheng, H. Zhang, Y. Wang, H. Zhang, S. Yamaguchi, ESIPT-active organic compounds with white luminescence based on crystallization-induced keto emission (CIKE), *Chem. Commun.* 53 (2017) 7832-7835.
- [2] X. Ren, F. Wang, J. Lv, T. Wei, W. Zhang, Y. Wang, X. Chen, An ESIPT-based fluorescent probe for highly selective detection of glutathione in aqueous solution and living cells, *Dyes Pigm.* 129 (2016) 156-162.
- [3] L. Tang, X. Dai, K. Zhong, D. Wu, X. Wen, A novel 2,5-diphenyl-1,3,4-oxadiazole derived fluorescent sensor for highly selective and ratiometric recognition of  $\text{Zn}^{2+}$  in water through switching on ESIPT, *Sens. Actuator. B* 203 (2014) 557-564.
- [4] H. M. Lv, Y. Chen, J. Lei, C. T. Au, S. F. Yin, An ESIPT-based ratiometric fluorescent probe for the imaging of nitroxyl in living cells, *Anal. Methods* 7 (2015) 3883-3887.
- [5] S. Barman, S. K. Mukhopadhyay, S. Biswas, S. Nandi, M. Gangopadhyay, S. Dey, A. Anoop, N. D. P. Singh, A p-hydroxyphenacyl-benzothiazole-chlorambucil conjugate as a real-time monitoring drug-delivery system assisted by excited state intramolecular proton transfer, *Angew. Chem.* 128 (2016) 4266-4270.
- [6] V. S. Padalkar, A. Tathe, V. D. Gupta, V. S. Patil, K. Phatangare, N. Sekar, Synthesis and photophysical characteristics of ESIPT inspired 2-substituted benzimidazole, benzoxazole and benzothiazole fluorescent derivatives, *J. Fluor.* 22 (2012) 311-322.
- [7] F. S. Rodembusch, F. P. Leusin, L. B. Bordignon, M. R. Gallas, New fluorescent monomers and polymers displaying an intramolecular proton-transfer mechanism in the electronically excited state (ESIPT) Part II. Synthesis, spectroscopic characterization and solvatochromism of new benzazolylvinylene derivatives. *J. Photochem. Photobiol. A: Chem.*, 173 (2005) 81-92.
- [8] J. Wiss, V. May, N. P. Ernsting, V. Farztdinov, A. Mühlfordt, Frequency and time-domain analysis of excited-state intramolecular proton transfer. Double-proton transfer in 2, 5-bis(2-benzoxazolyl)-hydroquinone. *Chem. Phys. Lett.* 346 (2001) 503-511.

- [9] K. Takagi, K. Ito, Y. Yamada, T. Nakashima, R. Fukuda, M. Ehara, H. Masu, Synthesis and optical properties of excited-state intramolecular proton transfer active  $\pi$ -conjugated benzimidazole compounds: influence of structural rigidification by ring fusion, *J. Org. Chem.* 82 (2017) 12173-12180.
- [10] S. Manoharan, S. Anandan, Cyanovinyl substituted benzimidazole based (DipeA) organic dyes for fabrication of dye sensitized solar cells, *Dyes Pigm.* 105 (2014) 223-231.
- [11] B. Zaifoglu, S. O. Hacioglu, N. A. Unlu, A. Cirpan, L. Toppare, Structure–property relations in donor–acceptor–donor type benzimidazole containing conjugated polymers, *J. Mater. Sci.* 49 (2014) 225-231.
- [12] E. Heyer, K. Benelhadj, S. Budzák, D. Jacquemin, J. Massue, G. Ulrich, On the fine-tuning of the excited-state intramolecular proton transfer (ESIPT) process in 2-(2'-hydroxybenzofuran)benzazole (HBBX) dyes, *Chem. Eur. J.* 23 (2017) 7324-7336.
- [13] R. Ali, R. C. Gupta, S. K. Dwivedi, A. Misra, Excited state proton transfer (ESIPT) based molecular probe to sense  $F^-$  and  $CN^-$  anions through fluorescence “Turn - On” response, *New J. Chem.* 42 (2018) 11746-11754.
- [14] E. Horak, P. Kassala, M. Hranjecb, I. M. Steinberg, Benzimidazole functionalised Schiff bases: Novel pH sensitive fluorescence turn-on chromoionophores for ion-selective optodes, *Sensors and Actuators B* 258 (2018) 415-423.
- [15] V. Kachwal, I. S. V. Krishna, L. Fageria, J. Chaudhary, R. K. Roy, R. Chowdhury, I. R. Laskar, Exploring the hidden potential of a benzothiazole-based Schiff-base exhibiting AIE and ESIPT and its activity in pH sensing, intracellular imaging and ultrasensitive & selective detection of aluminium ( $Al^{3+}$ ), *Analyst.* 143 (2018) 3741-3748.
- [16] J. Jayabharathi, V. Thanikachalam, K. Jayamoorthy, Effective fluorescent chemosensors for the detection of  $Zn^{2+}$  metal ion, *Spectrochim. Acta A* 95 (2012) 143-147.
- [17] K. Zhong, M. Cai, S. Hou, Y. Bian, L. Tang, A simple benzimidazole based fluorescent sensor for ratiometric recognition of  $Zn^{2+}$  in water, *Bull. Korean Chem. Soc.* 35 (2014) 489-493.
- [18] D. Jeyanthi, M. Iniya, K. Krishnaveni, D. Chellappa, A ratiometric fluorescent sensor for selective recognition of  $Al^{3+}$  ions based on a simple benzimidazole platform, *RSC Adv.* 3 (2013) 20984-20989.
- [19] J. Hu, J. Li, J. Qia, J. Chen, Highly selective and effective mercury (II) fluorescent sensors, *New J. Chem.* 39 (2015) 843-848.
- [20] W. Cao, X. Zheng, J. Sun, W. Wong, D. Fang, J. Zhang, L. Jin, A highly selective chemosensor for Al(III) and Zn(II) and its coordination with metal ions, *Inorg. Chem.* 53 (2014) 3012-3021.
- [21] S. K. Shoor, A. K. Jain, V. K. Gupta, A simple Schiff base based novel optical probe for aluminium (III) ions, *Sens. Actuators B* 216 (2015) 86-104.
- [22] K. Boonkitpatarakul, J. Wang, N. Niamnont, B. Liu, L. McDonald, Y. Pang, M. Sukwattanasinitt, Novel turn-on fluorescent sensors with mega stoke shifts for dual detection of Al and Zn, *ACS Sens.* 1 (2016) 144-150.
- [23] L. K. Kumawat, M. Asif, V. K. Gupta, Dual ion selective fluorescence sensor with potential applications in sample monitoring and membrane sensing, *Sens. Actuators B* 241 (2017) 1090-1098.

- [24] A. Jana, B. Das, S. K. Mandal, S. Mabhai, A. R. K. Bukhsh, S. Dey, Deciphering the liaison of CHEF-PET-ESIPT mechanism in a  $Zn^{2+}$  chemosensor and its applications in cell imaging study, *New J. Chem.* 40 (2016) 5976-5984.
- [25] B. K.Y. Bitanirwe, M. G. Cunningham, Zinc: The brain's dark horse, *Synapse* 63 (2009) 1029-1049.
- [26] S. Nandi, D. Das, Smart probe for multi-analyte signaling: solvent dependent selective recognition of I, *ACS Sens.* 1 (2016) 81-87.
- [27] M. P. Cuajungco, G. J. Lees, Zinc metabolism in the brain: relevance to human neurodegenerative disorders, *Neurobiol. Dis.* 4 (1997) 137-169.
- [28] L. He, B. Dong, Y. Liu, W. Lin, Fluorescent chemosensors manipulated by dual/triple interplaying sensing mechanisms, *Chem. Soc. Rev.* 45 (2016) 6449-6461.
- [29] M. J. Frisch, G. W. Trucks, H. B. Schlegel, G. E. Scuseria, M. A. Robb, J. R. Cheeseman, G. Scalmani, et al. GAUSSIAN 09 (Revision A.02), Gaussian Inc., Wallingford, CT, 2016.
- [30] D. W. Hein, R. J. Alheim, J. J. Leavitt, the use of polyphosphoric acid in the synthesis of 2-aryl- and 2-alkyl-substituted benzimidazoles, benzoxazoles and benzothiazoles, *J. Am. Chem. Soc.* 79 (1957) 427-429.
- [31] Y. Dong, R. Fan, W. Chen, P. Wang and Y. Yang, "A simple quinolone schiff-base containing chef based fluorescence 'turn-on' chemosensor for distinguishing  $Zn^{2+}$  and  $Hg^{2+}$  with high sensitivity, selectivity and reversible, *Dalton. Trans.*, 46 (2017) 6769-6775, 2017.
- [32] H. A. Benesi, J. H. Hildebrand, A spectrophotometric investigation of the interaction of iodine with aromatic hydrocarbons, *J. Am. Chem. Soc.* 71 (1949) 2703-2707.
- [33] T. Han, X. Feng, B. Tong, J. Shi, L. Chen, J. Zhi, Y. Dong, A novel "turn-on" fluorescent chemosensor for the selective detection of  $Al^{3+}$  based on aggregation-induced emission. *Chem. Commun.* 48 (2012) 416-418.
- [34] Guidelines for drinking-water quality, 2nd ed. Vol. 2. World Health Organization, Geneva, 1996.
- [35] A. K. Mahapatra, S. S. Ali, K. Maiti, S. K. Manna, R. Maji et al., Aminomethylpyrene-based imino-phenol as primary fluorescence switch-on sensors for  $Al^{3+}$  in solution and in vero cells and their complexes as secondary recognition ensemble toward pyrophosphate, *RSC Adv.* 5 (2015) 81203-81211.
- [36] M. J. Kim, K. Kaur, N Singh, D. Jang, Benzimidazole-based receptor for  $Zn^{2+}$  recognition in a biological system: a chemosensor operated by retarding the excited state proton transfer, *Tetrahedron* 68 (2012) 5429-5433.
- [37] Z. Tian, S. Cui, G Liu, R. Wang, S. Pu, A new fluorescent sensor for  $Zn^{2+}$  based on diarylethene with a 4-diethylaminosalicylaldehyde Schiff base unit, *J. Phys. Org. Chem.* 29 (2016) 421-429.